Biosensors and Bioelectronics ■ (■■■■) ■■■–■■■

Contents lists available at ScienceDirect

Biosensors and Bioelectronics

journal homepage: www.elsevier.com/locate/bios

An impedance immunosensor based on low-cost microelectrodes and specific monoclonal antibodies for rapid detection of avian influenza virus H5N1 in chicken swabs

Jianhan Lin [a,*], Ronghui Wang [b], Peirong Jiao [c], Yuntao Li [d], Yanbin Li [b], Min Liao [c], Yude Yu [d], Maohua Wang [e]

[a] MOA Key Laboratory of Agricultural Information Acquisition Technology (Beijing), China Agricultural University, Beijing 100083,China
[b] Department of Biological and Agricultural Engineering, University of Arkansas, Fayetteville, AR 72701, USA
[c] College of Veterinary Medicine, South China Agricultural University, Guangzhou, Guangdong 510642, China
[d] State Key Lab of Integrated Optoelectronics, Institute of Semiconductors, Chinese Academy of Science, Beijing 100083, China
[e] Modern Precision Agriculture System Integration Research Key Laboratory of Ministry of Education, China Agricultural University, Beijing 100083,China

ARTICLE INFO

Article history:
Received 6 June 2014
Received in revised form
20 August 2014
Accepted 10 September 2014

Keywords:
Impedance immunosensor
Avian influenza detection
Interdigitated array microelectrode
Asian in-field H5N1 virus

ABSTRACT

Early screening of suspected cases is the key to control the spread of avian influenza (AI) H5N1. In our previous studies, an impedance biosensor with an interdigitated array microelectrode based biochip was developed and validated with pure AI H5 virus, but had limitations in cost and reliability of the biochip, specificity of the antibody against Asian in-field H5N1 virus and detection of H5N1 virus in real samples. The purpose of this study is to develop a low-cost impedance immunosensor for rapid detection of Asian in-field AI H5N1 virus in chicken swabs within 1 h and validate it with the H5N1 virus. Specific monoclonal antibodies against AI H5N1 virus were developed by fusion of mouse myeloma cells with spleen cells isolated from an H5N1-virus-immunized mouse. Dot-ELISA analysis demonstrated that the developed antibodies had good affinity and specificity with the H5N1 virus. The microelectrodes were redesigned with compact size, fabricated using an improved wet-etching micro-fabrication process with a higher qualified production rate of 70–80%, and modified with the antibodies by the Protein A method. Equivalent circuit analysis indicated that electron transfer resistor was effective with the increase in impedance after capturing of the H5N1 viruses. Linear relationship between impedance change and logarithmic value of H5N1 virus at the concentrations from 2^{-1} to 2^{4} HAU/50 μl was found and the lower limit of detection was 2^{-1} HAU/50 μl. No obvious interferences from non-target viruses such as H6N2, H9N2, Newcastle disease virus, and infectious bronchitis virus were found. Chicken swab tests showed that the impedance immunosensor had a comparable accuracy with real-time RT-PCR compared to viral isolation.

1. Introduction

Avian influenza (AI) H5N1 has attributed to enormous economic loss and posed a potential pandemic threat to global human public health. AI virus outbreaks have been reported in more than 46 countries for animal cases and in 15 countries for human cases with 649 infections and 385 deaths since 2003 (WHO, 2014). Early screening of suspected cases is the key to effectively prevent and control the spread of this highly pathogenic AI virus. With new occurrences of Asian in-field AI H5N1 strains each year since 2008, there is an urgent need for simple, rapid, and low-cost methods for in-field detection of these H5N1 virus strains.

Currently available methods for detection of H5N1 virus mainly include viral isolation culture (gold standard method) (Woolcock, 2008; Bui et al., 2013), real-time Reverse Transverse Polymerase Chain Reaction (RT-PCR, WHO recommendation method) (WHO, 2007; Xie et al., 2006), and Enzyme Linked Immunosorbent Assay (ELISA) (Hemmatzadeh et al., 2013; Buehler et al., in press). However, these methods are not suitable for in-field screening of AI H5N1 now due to either time-consuming procedures, or complex sample pretreatment, or requirement of well-trained technicians and specialized facilities. As an alternative, biosensors have shown their potential to offer rapid, simple and sensitive detection to H5N1 virus. Recently, various types of biosensors were reported. Oh et al. developed an ion channel switch

* Corresponding author. Fax: +86 10 62737599.
E-mail address: jianhan@cau.edu.cn (J. Lin).

http://dx.doi.org/10.1016/j.bios.2014.09.037
0956-5663/

biosensor that could detect influenza A virus in clinical samples within 10 min after the sample was inoculated into chamber wells. This biosensor could obtain comparable results in sensitivity and reproducibility without sample pretreatment (Oh et al., 2008). A poly-silicon nanowire field-effect transistor was reported for specific and ultrasensitive detection of AI H5 virus DNA (Lin et al., 2009). The probe for capturing AI virus DNA was immobilized onto the poly-SiNW surface and the fM concentration level of target virus could be detected by measuring the *I–V* curve. Qi et al. (2010) described an imaging ellipsometric biosensor to identify H5N1 and H9N2 using a micro-array with multi-ligands. The immobilization of the antibodies was oriented onto a silicon wafer by means of the interaction between protein A and the Fc fragment of the antibody. Guo et al. (2013) fabricated an indium–tin-oxide (ITO) thin-film transistor on a glass substrate by a one-shadow-mask process to detect H5N1 virus. The monoclonal antibodies against H5N1 virus were immobilized on the ITO channel by (3-glycidoxypropyl)trimethoxysilane for specific capture of H5N1 virus. The negatively charged H5N1 viruses resulted in an increase in resultant threshold voltage and a decrease in field-effect mobility related to the concentration of H5N1 virus. A three-dimensional magnetic bead based microfluidic chip was also reported for electrochemical detection of inactivated H5N1 virus labeled with CdS quantum dots (Krejcova et al., 2014). However, these biosensors are still in lab research and many are not practical for use in the field.

Impedance biosensors, which depend on the measurement of the electrochemical impedance change on the interface of an electrode under an AC perturbation with a DC bias, have advantages over the conventional methods for biological detection, such as compact design, rapid detection, relatively low cost and ease to integration (Pejcic et al., 2006; Daniels and Pourmand, 2007). Different from other electrochemical methods which generally rely on costly electrochemical analyzers, impedance biosensors can be instrumented at low cost for practical applications since scanning at a range of frequencies to obtain the electrochemical impedance spectrum may be replaced with impedance measurement at a fixed characteristic frequency to obtain the impedance magnitude and phase angle, which is technically mature and commercially available. Besides, impedance biosensors are not influenced by the background color and surrounding lights compared to optical methods. Interdigitated array (IDA) microelectrodes are often used in the development of impedance biosensors due to their features of low ohmic drop, short detection time, high signal/noise ratio and small sizes (Varshney and Li, 2009; Lum et al., 2012). Besides, impedance biosensors can be easily integrated with immune magnetic separation, in which micro- or nano-sized magnetic beads modified with specific antibodies are used to efficiently capture the targets and then a magnetic field is applied to separate and concentrate the bead-target complexes, to obtain an improved sensitivity and specificity without requirements for expensive equipment and special training (Horak et al., 2007; Varshney et al., 2007).

In our previous studies, research work was focused on the proof-of-concept and prototype development of an impedance biosensor for detection of AI virus (Lum et al., 2012; Wang et al., 2009, 2011; Yan et al., 2013; Lin et al., 2010). The concept was proven using pure inactivated AI H5 virus and a research prototype with an IDA microelectrode based biochip was developed. However, the biochip was expensive due to the costly dry-etching fabrication process for fabrication of the high-quality IDA microelectrode and the low rate of qualified production in bonding the microelectrode with a micro-chamber. Besides, the high pressure in the biochip occasionally resulted in leakage from the biochip and damage to the microelectrode. More importantly, the antibodies used in the previously reported studies were not very specific to Asian in-field H5N1 virus strains, such as the AI H5N1 strain A/Duck/Guangdong/383/2008, which has been circulating widely in China since 2008 and may cause a new wave of cross-continental spreading from Asia to Europe. In this study, we developed an impedance immunosensor with an improved low-cost interdigitated array microelectrode and newly developed specific antibodies for rapid detection of Asian in-field H5N1 virus in chicken swabs.

2. Materials and methods

2.1. Materials

Phosphate buffered saline (PBS, 10 mM, pH 7.4) and Protein A (from *Staphylococcus aureus*) were purchased from Sigma-Aldrich (St. Louis, MO, USA). Bovine serum albumin (BSA) from EM Science (Gibbstown, NJ, USA) was prepared in PBS (1.0%, w/v) as blocking solution. AI virus subtypes H5N1 (A/Duck/Guangdong/383/2008), H6N2 (A/Chicken/Guangdong/C7/2009), and H9N2 (A/Chicken/Guangdong/HL/2006) as well as Newcastle disease virus (NDV) and infectious bronchitis virus (IBV) were provided by College of Veterinary Medicine, South China Agricultural University. The Western Blotting kit was purchased from KPL (Gaithersburg, MD, USA). Potassium ferricyanide, potassium ferrocyanide, sodium hydroxide and hydrochloric acid were purchased from Sinopharm Chemical Reagent Co., Ltd. (Shanghai, China). MilliQ water was produced by Advantage A10 from Millipore (Billerica, MA, USA) and used for preparation of all the solutions in this study.

2.2. Monoclonal antibody

Hybridoma cell strains were developed by fusion of SP2/0 mouse myeloma cells with spleen cells isolated from a BALB/C mouse, which was immunized with the purified AI H5N1 virus. Then, monoclonal antibody (MAb) cell strains for the H5 HA protein were determined by hemagglutinin inhibition (HI). HI titers of the H5 HA MAbs in the ascites were 9–11 log 2. The H5 HA MAbs in the ascites were purified by affinity column and stored at −80 °C. The H5 MAbs only reacted to AI subtype H5 virus and not to other AI subtype viruses by HI cross-reaction, which indicated the MAbs had good specificity to AI H5 virus.

2.3. Sample preparation

The strain of H5N1 virus was propagated in specific pathogen free (SPF) embryonating chicken eggs and titered as 10^3 EID_{50} /50 μl in chorioallantoic fluid. The prepared H5N1 viruses were diluted with vial transport media (2:3, v/v) and then used to inoculate Leghorn SPF chickens (0.1 ml for each chicken) via nasal and ocular routes of administration. Every day after inoculation, one tracheal swab and one cloacal swab were collected from each chicken and placed into separate sterile tubes with 1 ml PBS each. After vortexing for 10 s, the samples were placed at 4 °C for 3 min and the supernatants were pipetted. Eight swabs were pooled as one sample for test.

2.4. Microelectrode fabrication

The gold IDA microelectrodes were redesigned for the purpose of improving the fabrication quality and production rate. They were fabricated by an improved wet-etching method at the State Key Lab of Integrated Optoelectronics at the Institute of Semiconductor, Chinese Academy of Science. A 100 nm thick layer of gold (Au) was first evaporated on a glass wafer (10.16 cm in diameter, thoroughly rinsed prior to use) using a 10 nm thick layer of

Please cite this article as: Lin, J., et al., Biosensors and Bioelectronics (2014), http://dx.doi.org/10.1016/j.bios.2014.09.037

chromium (Cr) instead of titanium (Ti) as an adhesion layer because the adhesivity of Cr–Au is better than that of Ti–Au. Then, a positive photoresist was sputtered onto the Au layer and patterned by UV photolithography. Finally, an improved wet-etching method, in which an extra annealing process was applied at 400 °C for 20 s, was used to remove the unpatterned Au layer and the desired IDA microelectrodes were obtained. Each IDA microelectrode includes 25 pairs of digit electrodes with 15 μm digit width, 15 μm inter-digit spacing, and 3 mm digit length. The total area of the IDA microelectrode was ~77 mm^2 with a working area of ~4.5 mm^2 and 87 microelectrodes were fabricated per wafer with a qualified production rate of 70–80%.

2.5. Microelectrode modification

Immobilization of the antibodies on the IDA microelectrode surface was prepared by a three-step procedure. Prior to use, the microelectrodes were immersed in 1 M NaOH for 10 min and then 1 M HCl for 5 min. They were then softly wiped with pure ethanol and dried by nitrogen flow to remove contaminants. First, Protein A from *S. aureus*, which can absorb to gold surfaces in a non-specific way through electrostatic and hydrophobic interactions (Ferapontova et al., 2001), was prepared (1 mg/ml in PBS) and dropped onto the microelectrodes, followed by incubation for 45 min and washing with deionized water to remove surplus Protein A. Secondly, the immobilization of the monoclonal antibodies was achieved by dropping the antibodies (~0.2 mg/ml, 30 μl) onto the Protein A-modified surface and allowing them to incubate for 45 min. Protein A can specifically interact with the Fc fragment of the immunoglobulin (IgG) molecules of the antibodies (Guisan, 2006). After washing with deionized water to remove surplus antibodies, the antibody-modified surface was blocked using BSA in PBS solution (1.0%, w/v) for 30 min to avoid non-specific interactions. The microelectrodes were then washed thoroughly with deionized water to remove surplus BSA.

2.6. Impedance measurement

H5N1 virus detection was based on antigen-antibody immune reaction. The H5N1 viruses were captured by the monoclonal antibodies immobilized on the IDA microelectrode, which resulted in an increase of the impedance. 30 μl of sample with H5N1 virus was dropped onto the electrode, followed by incubation for 45 min and washing with deionized water. Then, the impedance spectrum of the electrode was measured using an impedance analyzer (E4980A, frequency response range: 20 Hz to 2 MHz, Agilent, Santa Clara, CA, USA) at a frequency range from 20 Hz to 1 MHz in the presence of $[Fe(CN)_6]^{3-/4-}$ redox probes. The individual concentrations of $[Fe(CN)_6]^{3-}$ and $[Fe(CN)_6]^{4-}$ are both 10 mM. The amplitude of the AC perturbation is 10 mV and the DC potential is 0 V. The impedance change was calculated as the difference between the impedance measured before and after the viruses were captured onto the electrodes.

2.7. Antibody evaluation

Dot-ELISA was used to evaluate the specificity and affinity between the developed antibody and AI virus subtypes (H5N1, H6N2 and H9N2) as well as other viruses (NDV and IBV). The detailed procedures of Dot-ELISA were described in a previously published paper (Lu, 2003).

3. Results and discussion

3.1. Evaluation of the monoclonal antibody

The affinity and specificity of the antibody directly impacts the sensitivity and specificity of the impedance immunosensor. Dot ELISA analysis was used to check the affinity between the antibody and Asian in-field subtype H5N1 virus and the cross reaction between the antibody and the non-target viruses. Both H5N1 virus (heat inactivated and methanol inactivated) and non-target viruses (H6N2, H9N2, NDV and IBV, all heat inactivated) were tested. The results are shown in Fig. 1. Both heat and methanol inactivated H5N1 virus produced visible dots at the concentrations from 2^{-1} to 2^5 HAU/50 μl, indicating that the antibody had good affinity with the H5N1 virus. No binding was found between the antibody and H6N2, and weak cross-reactions between the antibody and H9N2, NDV and IBV were observed.

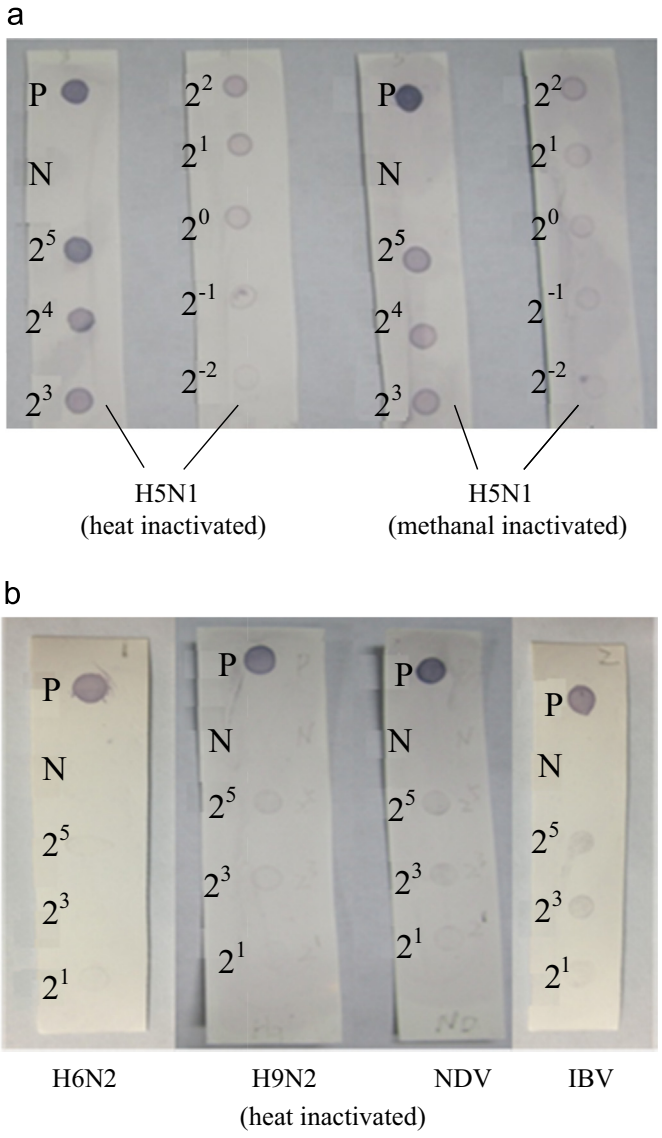

Fig. 1. (a) Dot-ELISA analysis on the affinity of the monoclonal antibody with H5N1 virus, (b) Dot-ELISA analysis on the cross-reactivity with H6N2, H9N2, NDV, and IBV.

Please cite this article as: Lin, J., et al., Biosensors and Bioelectronics (2014), http://dx.doi.org/10.1016/j.bios.2014.09.037

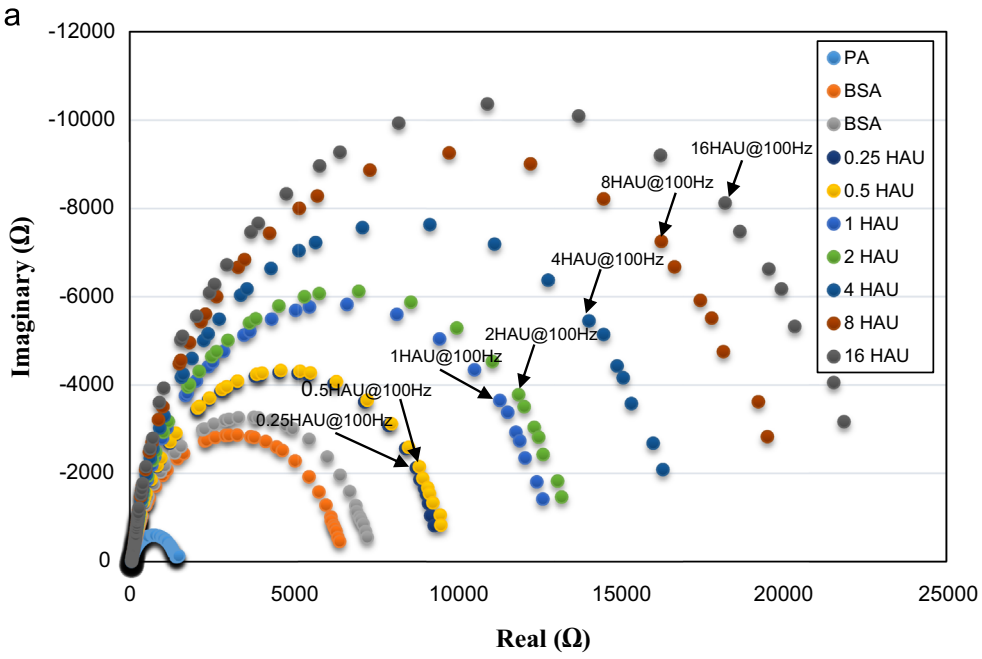

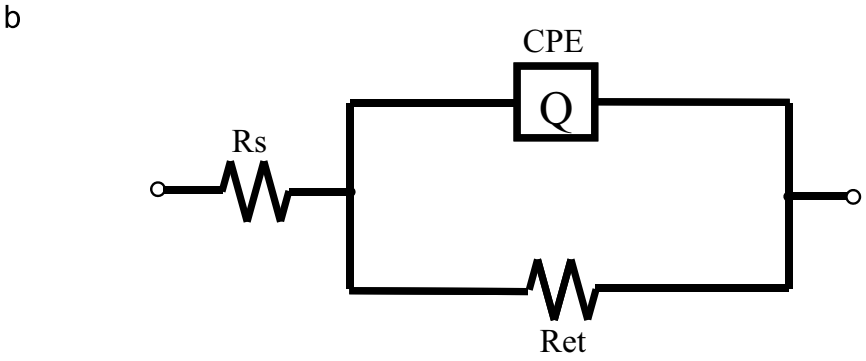

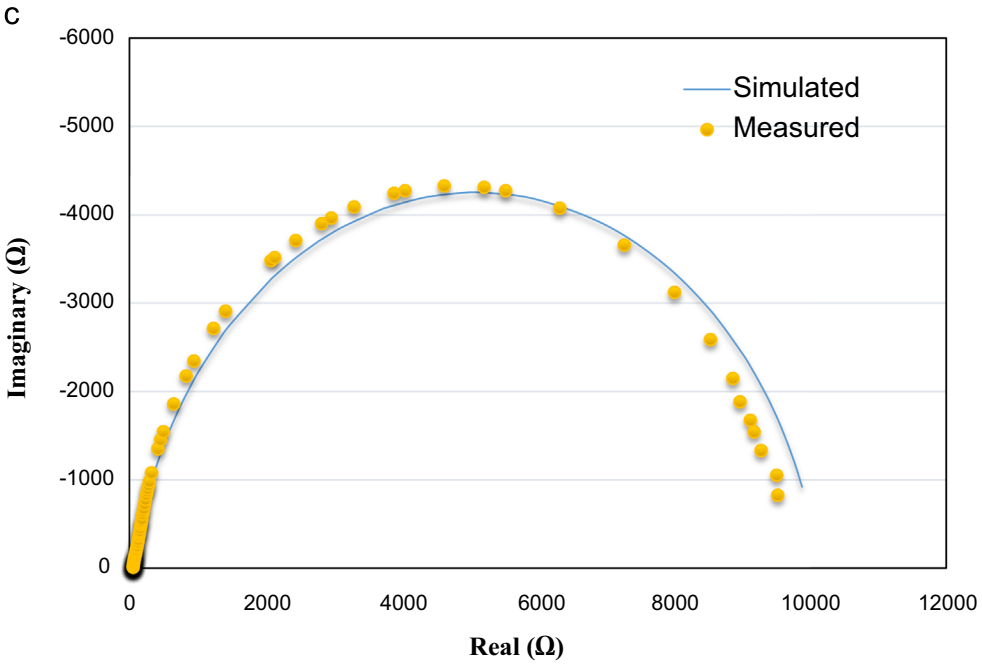

Fig. 2. (a) Nyquist diagram of measured impedance data taken from 2^{-1} to 2^{4} HAU/50 μl, (b) equivalent circuit for data analysis, including solution resistor (R_s), electron transfer resistor (R_{et}), and constant phase angle element (*CPE*), and (c) Nyquist diagram of measured impedance data and simulated impedance data taken at 2^{-1} HAU/50 μl.

3.2. Characterization of the impedance data

The impedance immunosensor is based on the measurement of Faradic current in the presence of $[Fe(CN)_6]^{3-/4-}$ as redox probes. This measurement of current is affected by the formation of biolayers on the electrode surface that block the electron transfer of the redox probe. The impedance spectrum for each step in the modification of the microelectrode and the detection of H5N1 virus at a frequency range of 20 Hz to 1 MHz were recorded as typical Nyquist plots and shown in Fig. 2(a). The binding of Protein A, antibody, BSA, and H5N1 virus onto the microelectrode's surface caused an increase in the impedance magnitude of the microelectrode sequentially.

For better understanding of the measured impedance data, a model shown in Fig. 2(b) was used as the equivalent circuit for simulation. The circuit includes three elements: solution resistor (R_s), constant phase angle element (*CPE*), and electron transfer resistor (R_{et}). R_s represents the resistance of the bulk electrolyte solution; *CPE* represents the charge separation at the electrode–solution interface; and R_{et} represents the resistance of the electron transfer of the redox probes. As shown in Table 1, when serial concentrations of H5N1 virus were measured, R_s had a slight change from −0.18% to 1.27%, *CPE* had a change from 14.25% to −26.21%, and R_{et} had a significant increase from 33.92% to 214.2%, indicating that electron transfer was more difficult. The reason for the higher value of R_{et} is that the surface is partially blocked, and actually this serves as one way to estimate the degree of surface coverage by the virus.

Fig. 2(c) shows the comparison between the measured impedance data and the simulated data generated using the equivalent circuit. The equivalent circuit was validated using the ZSimpWin software. The software selected 115 points from the measured impedance data to fit the simulated data. The mean relative standard deviation (RSD) of the impedance magnitude is 2.69% with a maximum RSD of 5.44%. Besides, the errors of R_s, *CPE*, and R_{et} obtained from the software are 0.91%, 2.81% and 1.21%, respectively.

3.3. Linearity of the immunosensor

The frequency range of 20–100 Hz was found to have obvious impedance changes in the detection of H5N1 virus. Triplicates were performed for each concentration in the range of 2^{-2}–2^4 HAU/50 µl. The mean RSD of the electrochemical impedance spectra experiments is 2.1% with a maximum RSD of 2.9%. The impedance magnitude measured at the characteristic frequency of 100 Hz was plotted for each step in the procedure of H5N1 virus detection. The impedance changes for the virus concentrations from 2^{-2} to 2^4 HAU/50 µl were $1992 \pm 34\ \Omega$, $2086 \pm 56\ \Omega$, $4870 \pm 123\ \Omega$, $5457 \pm 343\ \Omega$, $8048 \pm 234\ \Omega$, $10{,}781 \pm 424\ \Omega$ and $12{,}920 \pm 398\ \Omega$, respectively. The mean RSD of the impedance changes at different concentrations was 3.30% with a maximum RSD of 6.29%. As shown in Fig. 3, linear relationship between impedance change and logarithmic value of H5N1 virus concentration was found in the range of 2^{-1}–2^4 HAU/50 µl and can be described as $\Delta Z = 1905.7 \log_2 N - 1030.4$ ($R^2 = 0.96$). The lower limit of detection of this impedance immunosensor was determined based on signal to noise ratio ≥ 3, i.e. maximum standard deviation of the control measurements × 3, and was found to be 2^{-1} HAU/50 µl, which is lower than that of the previously developed immunosensor (2^0 HAU/50 µl) using different IDA microelectrodes and anti-H5 antibodies (Yan et al., 2013).

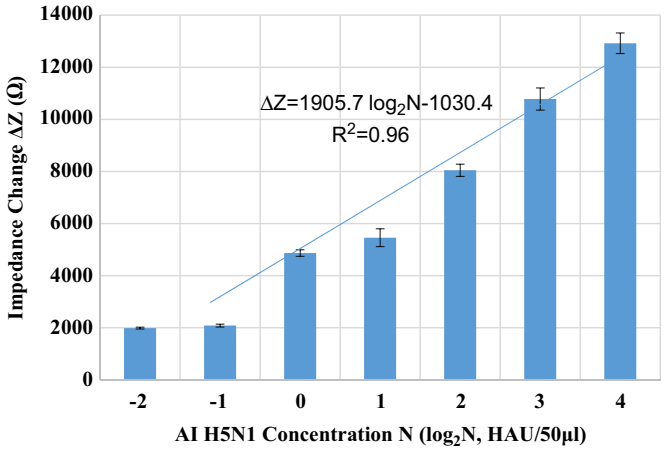

Fig. 3. Linear relationship between impedance change (ΔZ) measured at 100 Hz and logarithmic value of H5N1 virus concentration (N).

The total detection time was less than 1 h, which was less than or consistent with the previously reported immunosensor (Lum et al., 2012; Wang et al., 2009, 2011; Yan et al., 2013; Lin et al., 2010), and the most part of detection time was spent on the immune reaction between the viruses and the antibodies. The cost of the IDA microelectrodes fabricated in a small-scale production was significantly reduced due to the new compact design to obtain higher electrode production on the wafer with a diameter of 10.16 cm and the improved wet-etching micro-fabrication method to obtain higher quality of the electrode. Besides, the electrodes could be reused for ~5 times after thorough clean by NaOH and HCl, but it would be a challenge for recycling the electrodes in practical applications. The microelectrodes are very promising for further reduced cost in a mass production using larger-size wafer.

3.4. Specificity of the immunosensor

The specificity of this immunosensor is mainly dependent on the monoclonal antibodies against H5N1 virus, which were immobilized on the microelectrode's surface. False positive results caused by cross-reactivity and non-specific binding were of main concern. In a previous study (Yan et al., 2013), non-target viruses, including AI H9N2 virus and NDV, were used to test the specificity

Table 1
Contribution of the elements in the equivalent circuit to the impedance change in the detection of serial concentrations of H5N1 virus.

H5N1 Concentration (HAU/50 µl)	ΔR_s[a] (Ω cm^2)	$\Delta R_s/Rs$ (%)	ΔCPE[a] (S s^n/cm^2)	$\Delta CPE/CPE$ (%)	ΔR_{et}[a] (Ω cm^2)	$\Delta R_{et}/R_{et}$ (%)
2^{-1}	0.3	0.54	0.24×10^{-8}	2.76	2553	33.92
2^0	−0.1	−0.18	1.24×10^{-8}	14.25	6313	83.87
2^1	0.3	0.54	-0.17×10^{-8}	−1.95	6753	89.72
2^2	0.5	0.91	-0.20×10^{-8}	−2.30	10,403	138.21
2^3	0.6	1.09	-1.16×10^{-8}	−13.33	13,933	185.11
2^4	0.7	1.27	-2.28×10^{-8}	−26.21	16,123	214.20

[a] ΔR_s, ΔCPE and ΔR_{et} were calculated by subtract R_s, *CPE* and R_{et} simulated values after BSA blocking from those after some concentration of H5N1 virus capturing, respectively.

Please cite this article as: Lin, J., et al., Biosensors and Bioelectronics (2014), http://dx.doi.org/10.1016/j.bios.2014.09.037

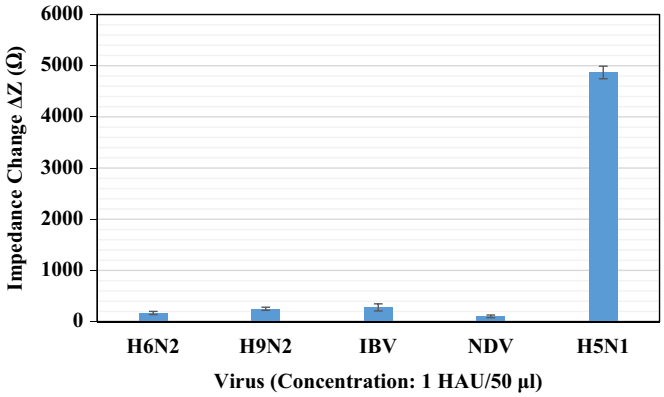

Fig. 4. Changes in impedance magnitude for detection of target and non-target viruses measured at 100 Hz. The concentration of H5N1 virus and the non-target viruses was 2^0 HAU/50 µl. Duplicate tests were conducted for each test.

Table 2
Comparison of viral isolation, real-time RT-PCR and this immunosensor in detection of AI H5N1 virus in chicken swabs.

Sample ID	Viral isolation	Real-time RT-PCR	Impedance immunosensor
Day 1–1	−	±	+
Day 1–2	−	−	−
Day 1–3	−	±	+
Day 1–4	−	−	−
Day 1–5	−	−	−
Day 2–1	+	+	+
Day 2–2	+	+	+
Day 2–3	+	+	+
Day 2–4	+	+	+
Day 2–5	+	+	+
Day 2–6	+	+	+
Day 3–1	+	+	+
Day 3–2	+	+	+
Day 3–3	+	+	+
Day 3–4	+	+	+
Day 3–5	+	+	+
Day 4–1	+	+	+
Day 4–2	+	+	+
Day 4–3	+	+	+
Day 4–4	+	+	+
Day 4-5	+	+	+

"+": positive; "−": negative; "±": weak positive.

of the immunosensor and the mean impedance change of H9N2 and NDV was ~10% of that of H5N1 at the same concentration.

In this study, more non-target viruses, including IBV, NDV, and AI subtypes H6N2 and H9N2, were used to evaluate the specificity of this immunosensor. The characteristic frequency of 100 Hz was used for impedance measurement and the same concentration (2^0 HAU/50 µl) of the non-target viruses and H5N1 virus were used for the specificity tests. As shown in Fig. 4, the impedance changes resulting from the non-target viruses were negligible ($168 \pm 30\ \Omega$ for H6N2, $250 \pm 30\ \Omega$ for H9N2, $278 \pm 70\ \Omega$ for IBV and $102 \pm 26\ \Omega$ for NDV, respectively) compared to that resulting from H5N1 virus ($4869 \pm 123\ \Omega$). The mean impedance change of non-target viruses was only 4.1% of that of H5N1 virus when they were at the same concentration, indicating that this immunosensor was more specific against target virus than the previously developed immunosensor (Yan et al., 2013).

3.5. Detection of H5N1 in swabs

The tracheal and cloacal swabs were collected daily after the chickens were inoculated with Asian in-field H5N1 virus. Eight swabs were pooled as one and equally separated into three pieces for blind test by viral isolation, real-time RT-PCR (ABI 7500, Applied Biosystems, Carlsbad, CA, USA) and this immunosensor, respectively. The threshold of the impedance immunosensor is a key to minimize the false positive and false negative ratio in the determination of the presence of H5N1 viruses in the real swabs and it was set as lower limit of detection of the immunosensor in this study.

The result of blind tests is shown in Table 2. In the first day's swab tests, both real-time RT-PCR and this impedance immunosensor had two positives while the gold standard method, viral isolation, did not show any positive for H5N1 virus. This might be because the threshold of the impedance immunosensor was set at a very low value. In the following days' tests, when the concentration of H5N1virus in the swabs became higher, three methods got the same positive results. The results of this blind test indicated that this impedance immunosensor had an accuracy of ~90% in chicken swab testing using viral isolation as a benchmark and it was comparable with real-time RT-PCR.

4. Conclusions

The purpose of this study was to develop a lower-cost impedance immunosensor for detection of Asian in-field subtype H5N1 virus in chicken swabs within 1 h. The cost of the interdigitated array microelectrode was significantly reduced due to more efficient electrode production using an improved wet-etching process instead of the high-cost dry-etching process and a new compact electrode design to increase microelectrode production. Specific antibody against H5 virus was successfully developed with good affinity and specificity with Asian in-field subtype H5N1 virus. Linear relationship between the impedance change at 100 Hz and the logarithmic value of H5N1 virus concentration from 2^{-1} to 2^4 HAU/50 µl were obtained. No obvious interference was found from non-target viruses such as H6N2, H9N2, NDV, and IBV. Compared with the previously reported immunosensor (Yan et al., 2013), this impedance immunosensor has a comparable sensitivity, better specificity against Asian in-field H5N1 virus, and a much lower cost. This immunosensor is an important step in developing a simple, rapid, robust, cost-effective, and reliable detection method.

Acknowledgements

This study was supported by grants from the International Cooperation Fund of MOST of P.R. China (No. 2010DFA31000) and Chinese Universities Scientific Fund (Nos. 2013QJ050 and 2014RC013). The authors thank Zachary Callaway for English edition and correction.

Appendix A. Supplementary information

Supplementary data associated with this article can be found in the online version at http://dx.doi.org/10.1016/j.bios.2014.09.037.

References

Bui, V.N., Ogawa, H., Ngo, L.H., Baatartsogt, T., Abao, L.N.B., Tamaki, S., Saito, K., Watanabe, Y., Runstadler, J., Imai, K., 2013. Arch. Virol. 158, 451–455.
Buehler, J., Lager, K., Vincent, A., Miller, C., Thacker, E., Janke, B., 2014. J. Vet. Diagn. Invest. (in press).
Daniels, J.S., Pourmand, N., 2007. Electroanalysis 19 (12), 1239–1257.
Ferapontova, E.E., Grigorenko, V.G., Egorov, A.M., Börchers, T., Ruzgas, T., Gorton, L., 2001. Biosens. Bioelectron. 16, 147–157.

Guo, D., Zhuo, M., Zhang, X., Xu, C., Jiang, J., Gao, F., Wan, Q., Li, Q., Wang, T., 2013. Anal. Chim. Acta 773, 83–88.
Guisan, J.M., 2006. Methods in Biotechnology: Immoblization of Enzymes and Cells, second edition Humana Press Inc., Totowa, NJ.
Hemmatzadeh, F., Sumarningsih, S., Tarigan, S., Indriani, R., Dharmayanti, N., Ebrahimie, E., Igniatovic, J., 2013. PLoS One 8 (2), 1–9.
Horak, D., Babic, M., Mackova, H., Benes, M.J., 2007. J. Sep. Sci. 30 (11), 1751–1772.
Krejcova, L., Nejdl, L., Rodrigo, M., Zurek, M., Matousek, M., Hynek, D., Zitka, O., Kopel, P., Adam, V., Kizek, R., 2014. Biosens. Bioelectron. 54, 421–427.
Lin, C., Hung, C., Hsiao, C., Lin, H., Ko, F., Yang, Y., 2009. Biosens. Bioelectron. 24, 3019–3024.
Lum, J., Wang, R., Lassiter, K., Srinivasan, B., Abi-Ghanem, D., Berghman, L., Hargis, B., Tung, S., Lu, H., Li, Y., 2012. Biosens. Bioelectron. 38, 67–73.
Lin, J., Lum, J., Wang, R., Tung, S., Hargis, B., Lu, H., Berghman, L., Li, Y., 2010. A portable impedance biosensor instrument for rapid detection of avian influenza virus. In: Proceedings of the IEEE, SENSORS, pp. 1558–1563.
Lu, H., 2003. Avian Dis. 47, 361–369.
Oh, S.Y., Cornell, B., Smith, D., Higgins, G., Burrell, C.J., Kok, T.W., 2008. Biosens. Bioelectron. 23, 1161–1165.
Pejcic, B., De Marco, R., Parkinson, G., 2006. Analyst 131 (10), 1079–1090.
Qi, C., Tian, X., Chen, S., Yan, J., Cao, Z., Tian, K., Gao, G., Jin, G., 2010. Biosens. Bioelectron. 25, 1530–1534.
Varshney, M., Li, Y., 2009. Biosens. Bioelectron. 24 (10), 2951–2960.
Varshney, M., Li, Y., Srinivasan, B., Tung, S., 2007. Sens. Actuators B—Chem. 128, 99–107.
WHO, 2014. Human infection with avian influenza A(H5N1) virus-update. http://www.who.int/csr/don/2014_01_09_h5n1/.
Woolcock, P.R., 2008. Methods Mol. Biol. 436, 35–46.
WHO, 2007. Recommendations and laboratory procedures for detection of avian influenza A(H5N1) virus in specimens from suspected human cases. http://www.who.int/influenza/resources/documents/h5n1_laboratory_procedures/en/index.html.
Wang, R., Wang, Y., Lassiter, K., Li, Y., Hargis, B., Tung, S., Berghman, L., Bottje, W., 2009. Talanta 79, 159–164.
Wang, R., Lin, J., Lassiter, K., Srinivasan, B., Lin, L., Lu, H., Tung, S., Hargis, B., Bottje, W., Berghman, L., Li, Y., 2011. J Virol. Methods 178, 52–58.
Xie, Z., Pang, Y.S., Liu, J., Deng, X., Tang, X., Sun, J., Khan, M.I., 2006. Mol. Cell Probes 20 (3–4), 245–249.
Yan, X., Wang, R., Lin, J., Li, Y., Wang, M., An, D., Jiao, P., Liao, M., Yu, Y., Li, Y., 2013. Sens. Lett. 11 (6–7), 1256–1260.

Please cite this article as: Lin, J., et al., Biosensors and Bioelectronics (2014), http://dx.doi.org/10.1016/j.bios.2014.09.037